6086 *Inorg. Chem.* **2009**, *48*, 6086–6095
DOI: 10.1021/ic9004483

Inorganic Chemistry
Article

Cobalt(II) Sheet-Like Systems Based on Diacetic Ligands: from Subtle Structural Variances to Different Magnetic Behaviors

Oscar Fabelo,[†] Jorge Pasán,[†] Laura Cañadillas-Delgado,[†] Fernando S. Delgado,[†] Francesc Lloret,[‡] Miguel Julve,[‡] and Catalina Ruiz-Pérez*[,†]

[†]*Laboratorio de Rayos X y Materiales Moleculares, Departamento de Física Fundamental II, Facultad de Física, Universidad de La Laguna, Avenida Astrofísico Francisco Sánchez s/n, E-38204 La Laguna, Tenerife, Spain, and* [‡]*Instituto de Ciencia Molecular (ICMol)/Departament de Química Inorgànica, Universitat de València, Polígono La Coma s/n, 46980 Paterna (València), Spain*

Received March 9, 2009

The preparation, X-ray crystallography, and magnetic investigation of the compounds $[Co(H_2O)_2(phda)]_n$ (**1**), $[Co(phda)]_n$ (**2**), and $[Co(chda)]_n$ (**3**) [H_2phda = 1,4-phenylenediacetic acid and H_2chda = 1,1-cyclohexanediacetic acid] are described herein. The cobalt atoms in this series are six- (**1**) and four-coordinated (**2** and **3**) in distorted octahedral (CoO_6) and tetrahedral (CoO_4) environments. The structures of **1**−**3** consists of rectangular-grids which are built up by sheets of cobalt atoms linked through *anti-syn* carboxylate bridges, giving rise to either a three-dimensional structure across the phenyl ring (**1** and **2**) or to regularly stacked layers with the cyclohexyl groups acting as organic separators (**3**). The magnetic properties of **1**−**3** were investigated as a function of the temperature and the magnetic field. Ferromagnetic coupling between the six-coordinate cobalt(II) ions across the *anti-syn* carboxylate bridge occurs in **1** ($J = +1.2$ cm^{-1}) whereas antiferromagnetic coupling among the tetrahedral cobalt(II) centers within the sheets is observed in **2** and **3** [$J = -1.63$ (**2**) and -1.70 cm^{-1} (**3**)] together with a spin-canted structure in **3** giving rise a long-range magnetic ordering ($T_c = 7.5$ K).

Introduction

Polynuclear compounds of high-spin cobalt(II) ions bridged by carboxylate groups exhibit different magnetic behaviors depending on the bridging mode of the carboxylate and on its coordination number.[1−3] In general, significant antiferromagnetic interactions between the metal centers are mediated by the carboxylate bridge in the *syn-syn* and *anti-anti* coordination modes,[1] whereas weak magnetic interactions either ferro- or antiferromagnetic in nature are observed across the *anti-syn* bridging mode.[2,3] Other bridges such as the hydroxo- or carboxylate-oxo have been also studied, and these works have shown that the nature of the d^7-d^7 exchange coupling is mainly governed by the angle at the bridging oxygen atom (θ) being antiferromagnetic for θ near 180° and either antiferro- or ferromagnetic when θ is close to 90°.[4]

Correlations between the magnetic properties of molecule-based solids and their structure together with the nature of the chemical bond are useful for the design of new materials.[5] In this respect, recent results on metal organic frameworks (MOFs) constituted by organic−inorganic magnetic layers have shown that it is possible to vary chemically the interlayer spacing.[6]

*To whom correspondence should be addressed. E-mail: caruiz@ull.es.

(1) (a) Jia, H.-P.; Li, W.; Ju, Z.-F.; Zhang, J. *Eur. J. Inorg. Chem.* **2006**, 4264–4270. (b) Ghoshal, D.; Mostafa, G.; Maji, T.-K.; Zangrando, E.; Lu, T.-H.; Ribas, J.; Chaudhuri, N.-R. *New J. Chem.* **2004**, *28*, 1204–1213.

(2) (a) Kumagai, H.; Oka, Y.; Inoue, K.; Kurmoo, M. *J. Phys. Chem. Solids* **2004**, *65*, 55–60. (b) Rueff, J. M.; Masciocchi, N.; Rabu, P.; Sironi, A.; Skoulios, A. *Eur. J. Inorg. Chem.* **2001**, 2843–2848.

(3) (a) Delgado, F. S.; Sanchiz, J.; Ruiz-Pérez, C.; Lloret, F.; Julve, M. *CrystEngComm.* **2003**, *5*, 280–284. (b) Kumagai, H.; Oka, Y.; Inoue, K.; Kurmoo, M. *Dalton Trans.* **2002**, 3442–3446. (c) Lee, E. W.; Kim, Y. J.; Jung, D. K. *Inorg. Chem.* **2002**, *41*, 501–506.

(4) Goodenough, J. B. *Magnetism and Chemical Bonds*; Wiley-Interscience: New York, 1963.

(5) (a) Coronado, E.; Dunbar, K. R. *Inorg. Chem.* **2009**, *48*, 3293–3295. (b) Her, J.-H.; Stephens, P. W.; Ribas-Ariño, J.; Novoa, J. J.; Shum, W.; Miller, J. S. *Inorg. Chem.* **2009**, *48*, 3296–3307. (c) Stamatatos, T. C.; Christou, G. *Inorg. Cem.* **2009**, *48*, 3308–3322. (d) Dawe, L. N.; Shuvaev, K. V.; Thompson, L. K. *Inorg. Chem.* **2009**, *48*, 3323–3341. (e) Andruh, M.; Costes, J.-P.; Díaz, C.; Gao, S. *Inorg. Chem.* **2009**, *48*, 3342–3359. (f) Hoshino, N.; Ako, A. M.; Powell, A. K.; Oshio, H. *Inorg. Chem.* **2009**, *48*, 3396–3407. (g) Gatteschi, D.; Cornia, A.; Mannini, M.; Sessoli, R. *Inorg. Chem.* **2009**, *48*, 3408–3419. (h) Miyasaka, H.; Julve, M.; Yamashita, M.; Clérac, R. *Inorg. Chem.* **2009**, *48*, 3420–3437. (i) Hatlevik, O.; Buschmann, W. E.; Zhang, J.; Manson, J. L.; Miller, J. S. *Adv. Mater.* **1999**, *11*, 914–918. (j) Verdaguer, M. *Science* **1996**, *272*, 698–699. (k) Sato, O.; Iyoda, T.; Fujishima, A.; Hashimoto, K. *Science* **1996**, *272*, 704–705. (l) O'Connor, C. *Research Frontiers in Magnetochemistry*; World Scientific Publishers: Singapore, 1993. (m) *Magnetic Molecular Materials*; Gatteschi, D., Kahn, O., Miller, J. S., Palacio, F., Eds.; Kluwer: Dordrecht, The Netherlands, 1991. (n) Babel, D. *Comments Inorg. Chem.* **1986**, *5*, 285–320.

(6) (a) Rabu, P.; Rouba, S.; Laget, V.; Hornick, C.; Drillon, M. *J. Chem. Soc., Chem. Commun.* **1996**, *10*, 1107–1108. (b) Fujita, W.; Awaga, K. *Inorg. Chem.* **1996**, *35*, 1915–1917. (c) Rabu, P.; Rueff, J. M.; Huang, Z. L.; Angelov, S.; Souletie, J.; Drillon, M. *Polyhedron.* **2001**, *20*, 1677–1685. (d) *Magnetism: Molecules to Materials*; Rabu, P., Drillon, M., Awaga, K., Fujita, W., Sekine, T., Miller, J. S., Drillon, M., Eds.; Wiley−VCH: Weinheim, Germany, 2001; pp 357−378.

Published on Web 05/28/2009

Focusing on two-dimensional (2D) magnetic systems where the metal centers are bridged by carboxylate groups, it is well known that the ferro- or antiferromagnetic nature of the intralayer magnetic coupling is strongly dependent on the conformation of the M−O−C−O−M unit, as mentioned above. The presence of magnetic anisotropy, as in the case of six-coordinated high-spin cobal(II), enhances the interest in these materials from a magnetic point of view.[7] Thinking of the preparation of functional materials with applications in gas storage, heterogeneous catalysis, and magnetic devices,[8] the use of polycarboxylic acids with aromatic rings seems to be a good choice given their versatility as ligands and their remarkable ability to afford extended networks. Most of the work has been carried out with rigid polycarboxylate ligands such as those derived from the 1,4-benzenedicarboxylic[9] and 1,3,5-benzenetricarboxylic[10] acids. Studies of complex formation between transition metal ions and more flexible polycarboxylate ligands containing rings such as the deprotonated forms of the 1,4-phenylenediacetic (H_2phda) or 1,1-cyclohexanediacetic (H_2chda) acids are not so common.[11]

In this work we present the first examples of MOFs resulting from the assembly of cobalt(II) ions with the phda^{2-} and chda^{2-} ligands, namely, $[Co(H_2O)_2(phda)]_n$ (**1**), $[Co(phda)]_n$ (**2**), and $[Co(chda)]_n$ (**3**). **1** and **2** are three-dimensional (3D) compounds whereas **3** is a two-dimensional (2D) network. Curiously, six- (**1**) and four-coordinated (**2** and **3**) high-spin cobalt(II) ions with distorted octahedral (**1**) and tetrahedral (**2** and **3**) environments occur therein with ferro- (**1**) and antiferromagnetic (**2** and **3**) interactions between the magnetic centers. Interestingly, **3** is a spin canted antiferromagnet with T_c = 7.5 K. The preparation of **1**−**3** together with their X-ray structures and magnetic investigation as a function of the temperature are the subject of this paper.

(7) (a) Zhu, Z.; Karasawa, S.; Koga, N. *Inorg. Chem.* **2005**, *44*, 6004–6011. (b) Beghidja, A.; Hallynck, S.; Welter, R.; Rabu, P. *Eur. J. Inorg. Chem.* **2005**, 662–669. (c) Miyasaka, H.; Ieda, H.; Masamoto, N.; Sugiura, K.; Yamashita, M. *Inorg. Chem.* **2003**, *42*, 3509–3515.

(8) Themed issue: Metal−organic frameworks. (a) Long, J. R.; Yaghi, O. M. *Chem. Soc. Rev.* **2009**, *38*, 1213–1214. (b) O'Keeffe, M. *Chem. Soc. Rev.* **2009**, *38*, 1215–1217. (c) Spokoyny, A. M.; Kim, D.; Sumrein, A.; Mirkin, C. A. *Chem. Soc. Rev.* **2009**, *38*, 1218–1227. (d) Uemura, T.; Yanai, N.; Kitagawa, S. *Chem. Soc. Rev.* **2009**, *38*, 1228–1247. (e) Ma, L.; Abney, C.; Lin, W. *Chem. Soc. Rev.* **2009**, *38*, 1248–1256. (f) Tranchemontagne, D. J.; Mendoza-Cortés, J. L.; OKeeffe, M.; Yaghi, O. M. *Chem. Soc. Rev.* **2009**, *38*, 1257–1283. (g) Czaja, A. U.; Trukhan, N.; Muller, U. *Chem. Soc. Rev.* **2009**, *38*, 1284–1293. (g1) Murray, L. J.; Dincă, M.; Long, J. R. *Chem. Soc. Rev.* **2009**, *38*, 1294–1314. (h) Wang, Z.; Cohen, S. M. *Chem. Soc. Rev.* **2009**, *38*, 1315–1329. (i) Allendorf, M. D.; Bauer, C. A.; Bhakta, R. K.; Houk, R. J. T. *Chem. Soc. Rev.* **2009**, *38*, 1330–1352. (j) Kurmoo, M. *Chem. Soc. Rev.* **2009**, *38*, 1353–1379. (k) Férey, G.; Serre, C. *Chem. Soc. Rev.* **2009**, *38*, 1380–1399. (l) Perry, J. J.IV; Perman, J. A.; Zaworotko, M. J. *Chem. Soc. Rev.* **2009**, *38*, 1400–1417. (m) Zacher, D.; Shekhah, O.; Wöll, C.; Fischer, R. A. *Chem. Soc. Rev.* **2009**, *38*, 1418–1429. (n) Shimizu, G. K. H.; Vaidhyanathan, Ra.; Taylor, J. M. *Chem. Soc. Rev.* **2009**, *38*, 1430–1449. (o) Yong Lee, J.; Farha, O. K.; Roberts, J.; Scheidt, K. A.; Nguyen, S. T.; Hupp, J. T. *Chem. Soc. Rev.* **2009**, *38*, 1450–1459. (p) Han, S. S.; Mendoza-Cortés, J. L.; Goddard, W. A. III *Chem. Soc. Rev.* **2009**, *38*, 1460–1476. (q) Li, J.-R.; Kuppler, R. J.; Zhou, H.-C. *Chem. Soc. Rev.* **2009**, *38*, 1477–1504.

(9) Stepanow, S.; Lingenfelder, M.; Dmitriev, A.; Spillmann, H.; Delvigne, E.; Deng, X.; Cai, C.; Barth, J. V.; Kern, K. *Nat. Mater.* **2004**, *3*, 229–233.

(10) Rosi, N. L.; Eckert, J.; Eddaoudi, M.; Vodak, D. T.; Kim, J.; O'Keeffe, M.; Yaghi, O. M. *Science* **2003**, *300*, 1127–1129.

(11) (a) Babb, J. E. V.; Burrows, A. D.; Harrington, R. W.; Mahon, M. F. *Polyhedron* **2003**, *22*, 673. (b) Lin, X.; Wang, Y.-Q.; Cao, R.; Li, F.; Bi, W.-H. *Acta Crystallogr. C* **2005**, *61*, m292–m294. (c) Weng, C.-H.; Cheng, S.-C.; Wei, H.-M.; Wei, H.-H.; Lee, C.-J. *Inorg. Chim. Acta* **2006**, *359*, 2029–2040. (d) Chen, Z.-L.; Zhang, Y.-Z.; Liang, F.-P.; Wu, Q. *Acta Crystallogr, Sect.E: Struct. Rep. Online* **2006**, *62*, m2409–m2411.

Experimental Section

Materials and Methods. Reagents and solvents used in the syntheses of **1**−**3** were purchased from commercial sources and used without further purification. Elemental analyses (C, H, N) were performed with an EA 1108 CHNS/0 automatic analyzer. IR spectrum of **1** (4000−400 cm-1) was recorded on Bruker IF S55 spectrophotometer with the sample prepared as a KBr pellet.

Synthesis of the Complexes. $[Co(H_2O)_2(phda)]_n$ (1). An aqueous solution (5 mL) of cobalt(II) acetate tetrahydrate (0.125 g, 0.5 mmol) was poured dropwise into an aqueous solution (8 mL) of H_2phda (0.097 g, 0.5 mmol) under continuous stirring. The resulting mixture was sealed in a 23 mL stainless-steel reactor with a Teflon linear, and it was heated at 75 °C during 48 h. X-ray quality crystals of **1** as pink plates were obtained after cooling (no additional product has been obtained). Anal. Calcd for $C_{10}H_{12}CoO_6$ (**1**): C, 41.83; H, 4.21%. Found: C, 41.81; H, 4.18%. The IR spectrum of **1** shows a broad and intense peak at 3400 cm^{-1} (antisymmetric and symmetric OH stretching) which is consistent with the presence of coordinated water. The presence of phda accounts for a strong peak at 1580 cm^{-1} (ν_{as}COO), and medium intensities at 1437 and 1367 cm^{-1} (ν_sCOO), 813 and 738 cm^{-1} (δOCO).

$[Co(phda)]_n$ (2). An aqueous solution (8 mL) of cobalt(II) acetate tetrahydrate (0.250 g, 1 mmol) was added dropwise to another aqueous solution (15 mL) containing H_2phda (0.194 g, 1 mmol) under continuous stirring. The resulting mixture was sealed in a 45 mL stainless-steel reactor with a Teflon liner, and it was heated at 150 °C during 96 h. X-ray quality crystals of **2** as purple prisms were obtained after a fast cooling (no additional product has been obtained). Anal. Calcd for $C_{10}H_8CoO_4$ (**2**): C, 47.83; H, 3.21%. Found: C, 47.84; H, 3.19%. The IR spectrum of **2** exhibits strong peaks at 1565 (ν_{as}OCO) and 1449 and 1364 cm^{-1} (ν_sOCO) and medium intensity absorptions at 795 and 747 cm^{-1} (δOCO).

$[Co(chda)]_n$ (3). NaOH (0.80 g, 2 mmol) dissolved in distilled water (ca. 10 mL) was added to an aqueous solution (15 mL) of H_2chda (0.200 g, 1 mmol). An aqueous solution (8 mL) of $CoCl_2 \cdot 6H_2O$ (0.119 g, 0.5 mmol) was added dropwise to the previous one under continuous stirring. The resulting mixture was sealed in a 45 mL stainless-steel reactor with a Teflon liner, and it was heated at 170 °C during 96 h. Violet-pink plate-shape crystals of **3** were obtained after a fast cooling. The final product was washed with water and methanol and dried in air (no additional product has been obtained). Anal. Calcd for $C_{20}H_{28}Co_2O_8$ (**3**): C, 46.71; H, 5.49%. Found: C, 46.78; H, 5.46%. The IR of **3** exhibits characteristic bands for 1,1-cyclohexanediacetate. Strong absorption peaks at 1546 and 1423 cm^{-1} are assigned to ν_{as}OCO and ν_sOCO stretching vibrations of bidentate/bridging carboxylate groups.

Crystal Structure Determination and Refinement. Single crystal X-ray diffraction data sets were collected at 293(2) K (**1**−**3**) on a Nonius Kappa CCD diffractometer with graphite-monochromated Mo−K_α radiation (0.71073 Å). Orientation matrix and lattice parameters were determined by least-squares refinement of the reflections obtained by a $\theta-\chi$ scan (Dirac/lsq method). Data collection and data reduction of **1**−**3** were done with the COLLECT[12] and EVALCCD[13] programs. All the measured independent reflections were used in the analysis. The structures of **1**−**3** were solved by direct methods using the SHELXS97 computational program. All non-hydrogen atoms were refined anisotropically by the full-matrix least-squares technique based on F^2 using SHELXL97. The hydrogen atoms of **1**−**3** (except those of the water molecules) were positioned geometrically and refined with a riding model. The structures of **1**−**3** were solved by

(12) *DIRAX* Duisenberg, A. J. M. *J. Appl. Crystallogr.* **1992**, *25*, 92–96.

(13) *EVALCCD* Duisenberg, A. J. M.; Kroon-Batenburg, L. M. J.; Schreurs, A. M. M. *J. Appl. Crystallogr.* **2003**, *36*, 220–229.

Table 1. Crystal Data and Details of the Structure Determination for Complexes **1**−**3**

compound	**1**	**2**	**3**
formula	$C_{10}H_{12}CoO_6$	$C_{10}H_8CoO_4$	$C_{10}H_{14}CoO_4$
M	287.13	251.09	257.14
crystal system	monoclinic	monoclinic	orthorhombic
space group	$P2_1/a$	$P2_1/a$	$Pccn$
a, Å	8.7703(5)	9.6427(4)	6.2901(6)
b, Å	6.0112(5)	4.8841(2)	6.2901(9)
c, Å	9.7663(6)	19.6584(8)	25.864(4)
β, deg	100.886(5)	95.290(3)	-
V, Å^3	505.61(6)	921.89(7)	1023.3(2)
$\boldsymbol{Z}$	2	4	4
index ranges	$-8 < h < 11$	$-12 < h < 11$	$-8 < h < 6$
	$-7 < k < 7$	$-6 < k < 6$	$-7 < k < 6$
	$-10 < l < 12$	$-25 < l < 24$	$-22 < l < 33$
T (K)	293(2)	293(2)	293(2)
ρ_{calc} (Mg m^{-3})	1.886	1.809	1.669
λ (Mo-K$_\alpha$, Å)	0.71073	0.71073	0.71073
μ (Mo-K$_\alpha$, mm^{-1})	1.712	1.848	1.667
R_1, $I > 2\sigma(I)$ (all)	0.0340 (0.0495)	0.0357 (0.0461)	0.0542 (0.0847)
wR_2, $I > 2\sigma(I)$ (all)	0.0619 (0.0658)	0.0655 (0.0683)	0.1294 (0.1406)
measured reflections	2575	4765	3148
independent reflections (R_{int})	1150 (0.025)	2058 (0.026)	1036 (0.034)
crystal size	0.06 × 0.04 × 0.04	0.14 × 0.10 × 0.10	0.10 × 0.10 × 0.04

Table 2. Selected Bond Lengths (Å) and Angles (deg) for **1**[a]

Co(1)−O(1)	2.077(2)	Co(1)−O(1w)$^{(a\text{-}1)}$	2.101(2)
Co(1)−O(1)$^{(a\text{-}1)}$	2.077(2)	Co(1)−O(2)$^{(b\text{-}1)}$	2.122(2)
Co(1)-O(1w)	2.101(2)	Co(1)−O(2)$^{(c\text{-}1)}$	2.122(2)
O(1)−Co(1)−O(1w)	91.11(7)	O(1)−Co(1)−O(2)$^{(b\text{-}1)}$	94.96(7)
O(1)−Co(1)−O(1)$^{(a\text{-}1)}$	180.0	O(2)$^{(b\text{-}1)}$−Co(1)−O(2)$^{(c\text{-}1)}$	180.0
O(1w)$^{(a\text{-}1)}$−Co(1)−O(1w)	180.0		
Hydrogen Bonds			
D−H···A	d(D···A)	d(H···A)	<(D−H···A)
O(1w)−H(1wa)···O(2)$^{(a\text{-}1)}$	2.673(3)	1.89(4)	158(3)

[a] Symmetry codes: (*a-1*) = $-x+1,-y,-z+1$; (*b-1*) = $x-1/2,-y+1/2,z$; (*c-1*) = $-x+3/2,y-1/2,-z+1$.

direct methods using the SHELXS97[14] computational program. The hydrogen atoms in **1** and **2** were located in the calculated positions using the riding model (except those of the water molecules). For compound **1**, the hydrogen atoms of the coordinated water molecules were located from difference Fourier maps and refined with isotropic temperature factors. The chda^{2-} ligand in **3** is disordered into two different positions which were refined with coupled occupation factors, leading to sof values of 0.502 (11) and 0.498(11) for each conformation. Within each of these positions of the chda^{2-} ligand, the cyclohexyl groups have been encountered in two different conformations both refined with 0.5 occupation factor because they were generated by an 2-fold rotation axis. The location of the hydrogen atoms in **3** was precluded because of the high disorder of this structure. Although the cell parameters and the high symmetry of this disorder suggested the possibility to solve the structure in a different crystal system, such as the tetragonal one, the solutions obtained after thoroughly testing were not satisfactory.

The final geometrical calculations and the graphical manipulations were carried out with PARST97,[15] PLATON[16], and DIAMOND[17] programs. Their crystallographic data and the details of the refinements have been deposited at the Cambridge Crystallographic Data Centre with CCDC reference nos. 723126, 723127, and 723128, respectively. They are reported in a condensed form in Table 1.

Physical Characterizations. Magnetic susceptibility measurements on polycrystalline samples of compounds **1**−**3** were carried out in the temperature range 1.9−300 K with a Quantum Design SQUID magnetometer under different applied magnetic field ranged from 50 G to 1 T. The magnetization measurements were performed at 2.0 K in the field range ±5 T. Corrections for the diamagnetic contribution of the constituent atoms and for the magnetization of the sample holder were done.

Table 3. Selected Bond Lengths (Å) and Angles (deg) for **2**[a]

Co(1)−O(1)	1.956(2)	Co(1)−O(2)$^{(a\text{-}2)}$	1.951(2)
Co(1)−O(3)	1.956(2)	Co(1)−O(4)$^{(b\text{-}2)}$	1.968(2)
O(1)−Co(1)−O(2)$^{(a\text{-}2)}$	110.41(8)	O(2)$^{(a\text{-}2)}$−Co(1)−O(4)$^{(b\text{-}2)}$	111.15(7)
O(1)−Co(1)−O(3)	112.38(8)	O(3)−Co(1)−O(2)$^{(a\text{-}2)}$	111.49(7)
O(1)−Co(1)−O(4)$^{(b\text{-}2)}$	103.18(8)	O(3)−Co(1)−O(4)$^{(b\text{-}2)}$	107.91(7)

[a] Symmetry codes: (*a-2*) = $x, y+1, z$; (*b-2*) = $x-1/2,-y+3/2,z$.

Table 4. Selected Bond Lengths (Å) and Angles (deg) for **3**[a]

Co(1)−O(1)	1.965(4)	Co(1)−O(2A)	1.972(9)
		Co(1)−O(2B)	1.965(9)
O(1)−Co(1)−O(1)$^{(a\text{-}3)}$	111.5(2)	O(1)−Co(1)− O(2A)$^{(a\text{-}3)}$	101.0(3)
O(1)−Co(1)−O(2A)	123.0(3)	O(1)−Co(1)−O(2B)$^{(a\text{-}3)}$	122.7(3)
O(1)−Co(1)−O(2B)	101.0(3)	O(2A)−Co(1)−O(2A)	24.6 (4)

[a] Symmetry codes: (*a-3*) = $0.5-x, 0.5-y, z$.

Results and Discussion

Crystal Structures. The structures of the compounds **1**−**3** have been characterized by single crystal X-ray diffraction. Selected bond distances and angles together with the hydrogen bonds are listed in Tables 2 (**1**), 3 (**2**), and 4 (**3**).

(14) Sheldrick, G. M. *SHELXL-97: Program for the refinement of crystal structures from diffraction data*; University of Göttingen: Göttingen, Germany, 1997.
(15) Nardelli, M. *J. Appl. Crystallogr.* **1995**, *28*, 659–659.
(16) Spek, A. L. *J. Appl. Crystallogr.* **2003**, *36*, 7–13.
(17) *DIAMOND 2.1d*; Crystal Impact GbR: Bonn, Germany, 2000.

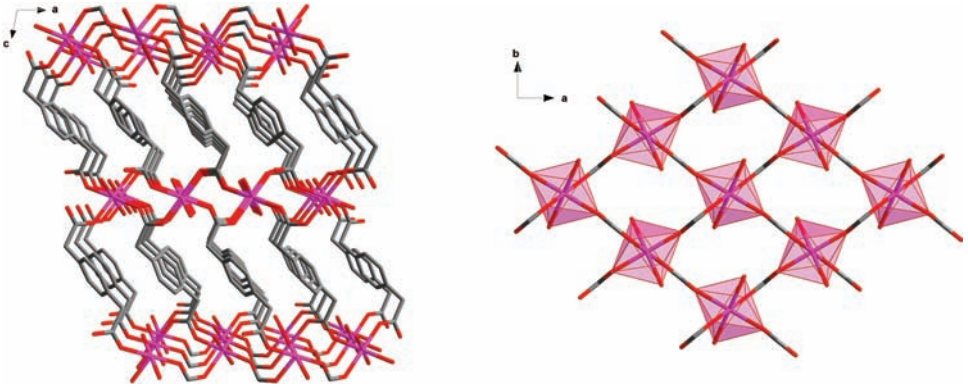

Figure 1. (Left) View along the *b*-axis of the crystal packing of **1** showing the interlayer connection through the skeleton of the phda^{2-} ligand. (Right) View along the *c*-axis of a fragment of the (4,4)-rectangular layer of cobalt atoms which are interlinked through *anti-syn* carboxylato bridges.

$[Co(H_2O)_2(phda)]_n$ (1). The structure of **1** is made up of (4,4)-rectangular layers parallel to the *ab* plane, with the $[Co(1)(H_2O)_2]^{2+}$ cations as 4-fold nodes connected through *anti-syn* carboxylate bridges from the fully deprotonated phda^{2-} groups (Figure 1, right). Each layer is connected to its two adjacent ones through the skeleton of the phda^{2-} ligand, giving rise to a 3D multilayered structure based on alternative stacking of (4,4) sheets pillared by the phenyl rings from the phenylenedicarboxylate ligands (Figure 1, left). Hydrogen bonding, involving the coordinated water molecules and oxygen atoms from carboxylate groups, contributes to the stabilization of the whole structure (see end Table 2).

The crystallographically independent cobalt atom [Co(1)] is located on an inversion center (Figure 2), and it is six-coordinated, in a slightly elongated octahedral environment, with geometric values ϕ and s/h of 59.28° and 1.23 (ideal values ϕ = 60° and s/h = 1.22).[18] The equatorial plane of Co(1) is built up by two water molecules and two carboxylate-oxygen atoms [O(1), O(1w), O(1)$^{a-1}$ and O(1w)$^{a-1}$; (*a-1*) = 1−*x*, −*y*, 1−*z*] whereas the axial positions are filled by another two carboxylate-oxygen atoms [O(2)$^{b-1}$ and O(2)$^{c-1}$; (*b-1*) = −0.5+*x*, 0.5−*y*, *z* and (*c-1*) = 1.5−*x*, −0.5+*y*, 1−*z*]. The mean value of the equatorial Co−O bond distance is 2.089(2) Å. This value is somewhat shorter than the average Co−O axial bond length [2.122(2) Å]. Each cobalt atom is connected to other four through four carboxylate groups that exhibit the *anti-syn* bridging conformation, giving rise to a (4,4) rectangular grid. These carboxylate groups act as connectors between equatorial and axial sites of each cobalt atom. Along each Co−O−C−O−Co pathway, the adjacent octahedra are tilted by 74.18°. This particular conformation is important to understand the ferromagnetic coupling observed in **1** (see below). The cobalt−cobalt separation through the *anti-syn* carboxylate bridge is 5.3164(4) Å [Co(1)···Co(1)$^{e-1}$; (*e-1*) = 1.5−*x*, 0.5+*y*, *1*−*z*], a value which is much smaller than the shortest separation between the metal atoms from two adjacent layers which are connected through the skeleton of the phda^{2-} group [10.3667(7) Å for Co(1)···Co(1)$^{d-1}$; (*d-1*) = 0.5−*x*, 0.5+*y*, −*z*].

Each phda^{2-} ligand in **1** is centrosymmetric, the inversion center being located in the middle of the phenyl ring. It adopts a tetrakis-monodentate coordination mode through its four carboxylate-oxygens: O(1) to Co(1), O(2) to Co(1)$^{e-1}$ and the corresponding symmetry-related atoms (Figure 2). The phda^{2-} group acts as a connector between adjacent (4,4) rectangular layers. Three geometrical parameters (noted θ, ψ, and φ in Scheme 1 are used in the literature[19] to describe the distortion degree of the phda^{2-} ligand: θ accounts for the bending in the center of the anion with the two carboxylate groups remaining coplanar, ψ represents the bending of the carboxylate groups toward each other,

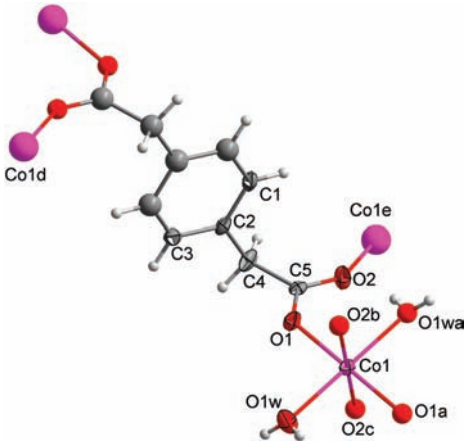

Figure 2. Perspective view of a fragment of the structure of **1** focusing on the coordination mode of the phda^{2-} ligand with the atom numbering. The crystallographically independent unit is outlined as an ORTEP representation (the thermal ellipsoids are drawn at the 50% probability level).

Scheme 1

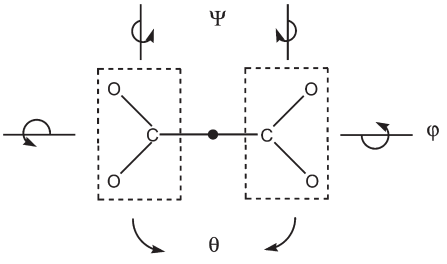

Scheme I

(18) Stiefel, E. I.; Brown, G. F. *Inorg. Chem.* **1972**, *11*, 434–436.

(19) Eddaoudi, M.; Kim, J.; Vodak, D.; Sudik, A.; Wachter, J.; O'Keeffe, M.; Yaghi, O. M. *Proc. Natl. Acad. Sci. U.S.A. 99*. **2002**, 4900-4904.

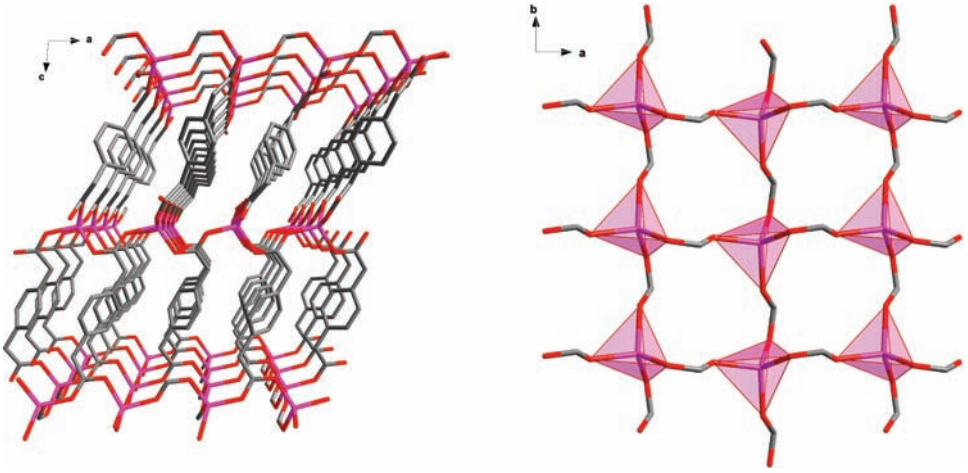

Figure 3. (Left) Central projection view along the *b* axis of the crystal packing of **2** showing the interlayer connection through the skeleton of the phda^{2-} ligand. (Right) View of a fragment of the (4,4) rectangular-grid layer of **2** which grows in the *ab* plane.

and φ is the relative twisting of the planes of two carboxylate groups. The θ, ψ, and φ, in the case of **1** are 180°, 180°, and 0°, respectively, values which are in agreement with those reported for other phda-containing metal complexes.[11a] The average value of the C−O bond lengths of the coordinated carboxylate-oxygen atoms is 1.277(2) Å. The internal C−C−C angles within the benzene ring at the substituted carbon atoms [117.7(2)°] are slightly smaller than those at the non-substituted ones [120.9(2)°], as expected.

We would like to finish this structural description of **1** with a brief comment on the structural similarities between **1** and the previously reported complex of formula $[Co(H_2O)_2(OOCCH_2OC_6H_5)_2]_n$ ($C_6H_5OCH_2$-COOH = phenoxyacetic acid).[20] This compound exhibits a square grid arrangement of cobalt(II) ions linked through *anti-syn* carboxylate bridges similar to that of **1**, but the layers in that compound are well separated from each other by the pendant phenyl rings, the shortest interlayer cobalt−cobalt separation being 16.9152(4) Å. The cobalt(II) is surrounded by two *trans*-coordinated water molecules and four carboxylate oxygen atoms building a somewhat elongated octahedral environment around the metal atom, as in **1**. The tilting between adjacent octahedra in the phenoxyacetate compound is 41.80°, a value which is slightly different from that observed in **1**.

[Co(phda)]$_n$ (2). The structure of **2** resembles that of **1** but the (4,4) rectangular-grid layers in **2** contain tetrahedral CoO_4 chromophores, *anti-syn* carboxylate bridges from the phda^{2-} ligand linking each cobalt atom, which acts as a 4-fold node. The (4,4) layers grow in the *ab* plane, and they are pillared along the *c* axis through the skeleton of two crystallographically independent phenylenediacetate ligands, building two sets of organic pillars, one above and one below each (4,4) network. The resulting 3D structure is based on a regular stacking which follows the *ABCDABCD* sequence, *A* and *C* being the inorganic and *B* and *C* the organic sheets. (Figure 3).

One crystallographically independent cobalt atom [Co(1)] occurs in **2**, and it is four-coordinated in a slightly distorted tetrahedral environment (see Table 3 and Figure 4). The mean Co−O bond distance is 1.958(2) Å, a value which is slightly shorter than those observed for the octahedral surrounding of the cobalt(II) ion in **1** [ca. 2.110(2) Å]. As in **1**, each cobalt atom in **2** is connected to other four metal atoms through four carboxylate bridges in the *anti-syn* conformation, giving rise to a (4,4) rectangular grid which grows in the *ab* plane. The tetrahedral $Co(1)O_4$ groups are tilted by 35.5° with respect to each other along the *a*-axis [angle calculated between two adjacent planes built up by O(3)−Co(1)−O(4)$^{b\text{-}2}$], this movement following an *ABAB* sequence (left/right). There is no significant twisting along the *b*-axis. The values of the cobalt−cobalt separations through the *anti-syn* carboxylate bridges are 4.8526(6) and 4.8841(5) Å across the O(3)−C(10)−O(4) and O(1)−C(5)−O(2) set of atoms, respectively. These values roughly correspond to the *a* and *b* crystallographic directions. The shortest separation between the cobalt atoms of two adjacent layers linked through the skeleton of the phda^{2-} ligand is 9.6520(6) Å, a value which is considerably much longer than those observed for the intralayer metal−metal separations.

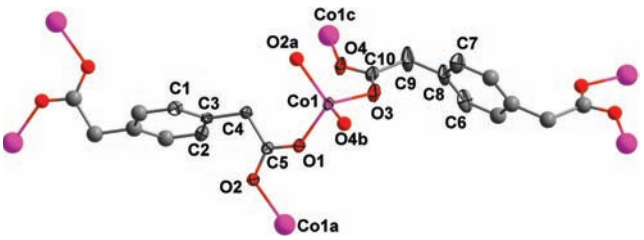

Figure 4. Perspective view of a fragment of the structure of **2** showing the tetrakis-monodentate coordination mode of the phda^{2-} ligand together with the atom numbering. The ORTEP representation has been used to denote the crystallographically independent unit (thermal ellipsoids are drawn at the 50% probability level).

Two crystallographically independent phda^{2-} ligands occur in **2**, and both are generated by an inversion center which is located in the middle of the phenyl rings. They adopt a tetrakis-monodentate coordination mode, similar to **1**, through the O(1), O(2), O(3), and O(4) atoms toward Co(1), Co(1)$^{a\text{-}2}$, Co(1), and Co(1)$^{c\text{-}2}$, respectively [symmetry code: (*a*-2) = x, $y-1$, z and (*c*-2) = $x+0.5$,

(20) Rueff, J.-M.; Paulsen, C.; Souletie, J.; Drillon, M.; Rabu, P. *Solid State Sci.* **2005**, *7*, 431–436.

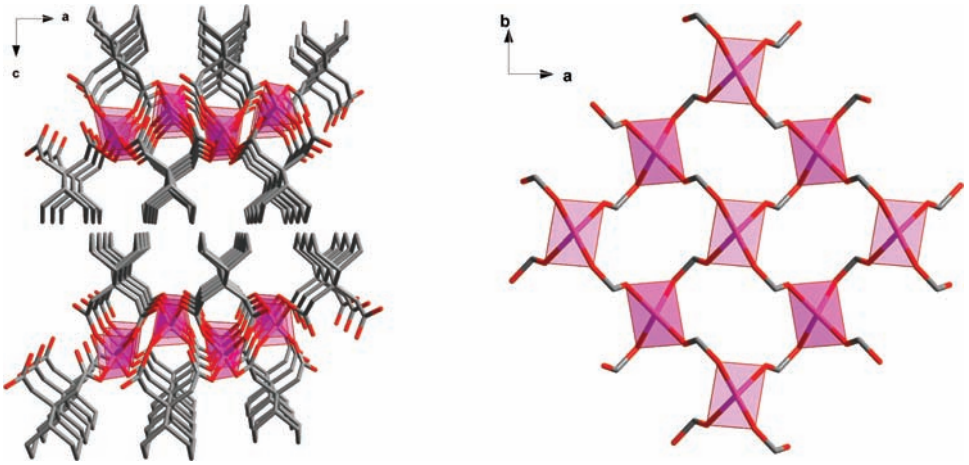

Figure 5. (Left) View of the crystal packing of **3** along the *c* axis showing how the cyclohexyl rings act as a hydrophobic barrier between the layers of Co(II) ions. (Right) View of a fragment of the (4,4)-square layer of cobalt atoms linked by *anti-syn* carboxylate groups which grows in the *ab* plane.

1.5−*y*, *z*], together with those symmetry-related (see Figure 4). The values of the θ, ψ, and φ parameters for both $(phda)^{2-}$ groups in **2** are the same than those observed in **1**. The average C−O bond length is 1.256(3) Å, a value which agrees very well with that observed in **1**. As expected, also the internal angles within the phenyl ring for the substituted carbon atoms are slightly smaller than those at the non-substituted ones [mean values 118.2(3) and 121.1(2)°, respectively].

The crystal structure of **2** is similar to that of **1**, the main difference concerning the cobalt(II) environment, octahedral in **1** with the inclusion of two water molecules but tetrahedral in **2**. Interestingly, the *c* unit cell parameter in **2** is twice longer than in **1**. This is due to the occurrence of two crystallographically independent $phda^{2-}$ ligands in **2** with two different layers of organic pillars, which also accounts for the two slightly different values of the shortest Co···Co separation through the two different organic layers in **2** [the distances being 9.6520(6) and 10.6678(6) Å].

As far as we know, only two previous examples of layers of tetrahedrally coordinated cobalt(II) ions have been reported, both of them containing dicarboxylate ligands, namely, $\{Co[O_2C(CH_2)_5CO_2]\}_n$[21] and $\{Co[O_2C(CH_2)_3CO_2]\}_n$[22] [$HO_2C(CH_2)_nCO_2H$ = pimelic (n = 5) and glutaric (n = 3) acids]. Both compounds exhibit a square grid arrangement of cobalt(II) ions linked through *anti-syn* carboxylate bridges. The Co(II) ions are surrounded by four carboxylate-oxygen atoms in a somewhat distorted tetrahedral environment. The values of the tilting between adjacent tetrahedral are 40.4° and 44.4° for the pimelate and glutarate complexes, respectively (calculated as for **1**). They are very close to those observed in **2**. The resulting 3D structure is, as occurs in **2**, also based on a regular stacking of inorganic (*A* and *C*) and organic sheets (*B* and *D*), which follow the *ABCDABCD* sequence, the two different interlayer cobalt−cobalt separations being 10.143(5) and 10.575(5) Å (pimelate complex) and 8.427(2) and 8.75(2) Å (glutarate compound).

$[Co(chda)]_n$ (3). The structure of **3** is built up from corrugated (4,4) square grid layers of cobalt atoms which act as 4-fold nodes being connected through *anti-syn* carboxylate bridges from the fully deprotonated $chda^{2-}$ ligand. These layers grow in the *ab* plane, and they are separated from each other along the *c* direction by the cyclohexyl groups of the $chda^{2-}$ ligands which act as a hydrophobic barrier between the inorganic sheets (Figure 5). There are two disordered positions for each dicarboxylate ligand and then, multiple scenarios are envisaged with the *A* and *B* conformations being randomly distributed within the crystal (Figure 6). This situation does not alter the overall structure described above but the local distortion at the $chda^{2-}$ ligand and at the cobalt environment.

One crystallographically independent cobalt atom [Co(1)] occurs in **3**, laying on a 2-fold rotation axis. As in **2**, each cobalt atom in **3** is four-coordinated in a slightly distorted tetrahedral environment, regardless of the *A* or *B* conformation of the dicarboxylate ligand. The mean value of the Co−O bond distance is 1.969(7) Å (see Table 4), a value which agrees with that observed in **3**. The position of the cobalt ions is fixed whatever the ligand conformation was. The Co···Co separation through the *anti-syn* carboxylate bridge is 4.6806(6) Å, and the angle among three-adjacent cobalt atoms is 143.75° (which defines the corrugation of the layer). The tetrahedral CoO_4 units in **3** are twisted as observed in **2**, with a tilt angle of 16.20°. The shortest interlayer cobalt−cobalt separation is 12.932(2) Å, a value which is much longer than the intralayer one.

One crystallographically independent $chda^{2-}$ ligand occurs in **3**. It is disordered into two different conformations, *A* and *B* [see Figure 6 (left)], with occupation factors of 0.502(11) and 0.498(11), respectively. Within each conformation, the cyclohexyl group is disordered into two positions of equal occupation since they are generated by a 2-fold rotation axis which corresponds to the vector connecting the C(1) carbon atom of the cyclohexyl ring and the cobalt atom Co(1), exhibiting a chair conformation. The $chda^{2-}$ group simultaneously adopts bidentate [through O(1) and $O(1)^{a-3}$ chelating Co(1) the angle subtended at the cobalt atom being 111.45(14)°] and bis-monodentate [through O(2A-B)

(21) Livage, C.; Edgger, C.; Nogues, M.; Férey, G. *C. R. Acad. Sci., Ser. Iic: Chim.* **2001**, *4*, 221–226.
(22) EunWon, L.; YooJin, K.; Dunk-Young, J. *Inorg. Chem.* **2002**, *41*, 501–506.

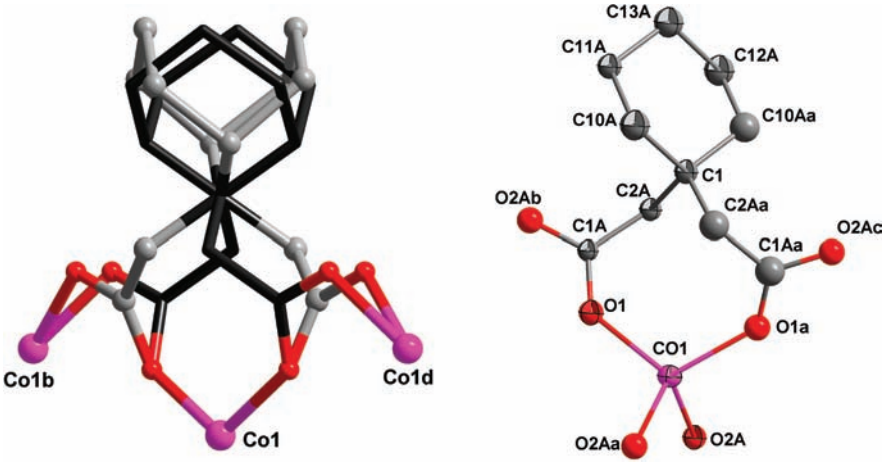

Figure 6. (Left) Two refined positions (*A*, gray and *B*, black) of the $chda^{2-}$ ligand in **3** showing its coordination mode. (Right) View of a fragment of the structure of **3** with the atom numbering (the ORTEP representation has been used to denote the crystallographically independent unit and only one position of the disordered cyclohexyl group has been drawn for the sake of clarity).

toward $Co(1)^{b\text{-}3}$ and $O(2A\text{-}B)^{c\text{-}3}$ toward $Co(1)^{d\text{-}3}$] coordination modes [symmetry code: (*b*-3) = $x-0.5,-y,0.5-z$; (*c*-3) = $1-x, 0.5+y, 0.5-z$; (*d*-3) = $x+0.5,1-y,0.5-z$]. The eight-member chelate ring formed by the bidentate coordination has been observed in the mononuclear manganese(II) complex $[Mn(phen)(H_2O)_2(chda)]\cdot 3H_2O$ (phen = 1,10-phenanthroline) which is the only previously reported chda-containing coordination compound.[23]

The main difference between the (4,4) layers of **2** and **3** is the corrugation occurring in **3**. All the cobalt atoms within each sheet of **2** are coplanar whereas those of **3** are located above or below its four nearest neighbors like an egg crate [the separation from the mean plane being 0.7288(8) Å].

Magnetic Properties

Compound 1. The magnetic properties of **1** in the form of the $\chi_M T$ product against T [χ_M being the magnetic susceptibility per mol of Co(II) ions] are shown in Figure 7. $\chi_M T$ smoothly decreases when cooling from room temperature [2.95 $cm^3\ mol^{-1}$ K at 295 K (μ_{eff} = 4.85 μ_B)] to reach a minimum at 30 K (ca. 2.49 $cm^3\ mol^{-1}$ K), and it increases sharply at lower temperatures to attain a value of 12.36 $cm^3\ mol^{-1}$ K at 1.9 K (under an applied magnetic field of 250 G). The decrease of $\chi_M T$ in the high temperature range is due to the depopulation of the high energy Kramers doublets (spin−orbit coupling effects) as expected for six coordinated high-spin cobalt(II) complexes. The increase of $\chi_M T$ in the low temperature region is due to a ferromagnetic exchange interaction between the Co(II) ions. This is supported by the fact that the value of $\chi_M T$ at the minimum (2.49 $cm^3\ mol^{-1}$ K) is well above that calculated for a magnetically isolated cobalt(II) ion (1.73 $cm^3\ mol^{-1}$ K for a S_{eff} = 1/2 with $g \approx 4.3$).[24] The lack of out-of-phase signal in the ac susceptibility down to 1.9 K precludes any magnetic ordering above this temperature.

When the large metal−metal separation through the skeleton of the ligand and the lack of exchange coupling between Co(II) ions in previous benzene-containing ligands as bta-bridged cobalt(II) complexes (H_4bta = 1,2,4,5-benzenetetracarboxylic acid) are considered,[25] the magnetic behavior of **1** would correspond to the (4,4) rectangular-grid layers of cobalt(II) ions linked through *anti-syn* carboxylate groups. The ferromagnetic coupling involved in **1** is observed at low temperatures (T < 29 K in Figure 7), just in the region where the ground-state Kramers doublet is the only populated state. This ground state can be treated as an effective spin doublet S_{eff} = 1/2 with a Landé factor $g_o = (10 + 2\alpha)/3$.[26]

To determine the value of the exchange interaction in **1** in the whole temperature range, we have used an

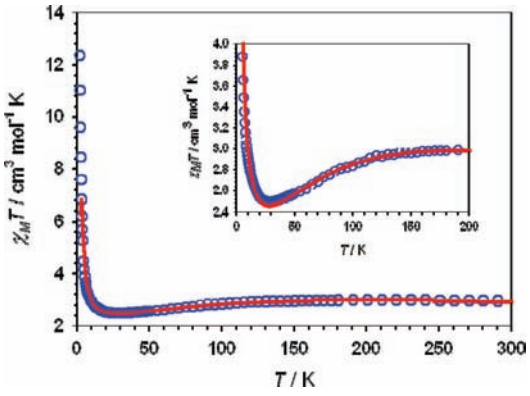

Figure 7. Temperature dependence of the $\chi_M T$ product of **1**: (blue circles) experimental data; (solid red line) best-fit curve through eq 1 (see text). The inset shows a detail of the region in the vicinity of the minimum of $\chi_M T$.

(23) Shen, L.; Yan, L.-C.; Jin, Z.-M.; Zhang, Y.-J. *Acta Crystallogr., Sect. E.* **2005**, *61*, m1419–m1421.
(24) Lines, M. E. *J. Chem. Phys.* **1971**, *55*, 2977–2984.

(25) (a) Fabelo, O.; Pasán, J.; Lloret, F.; Julve, M.; Ruiz-Pérez, C. *CrystEngComm* **2007**, *9*, 815–827. (b) Fabelo, O.; Pasán, J.; Lloret, F.; Julve, M.; Ruiz-Pérez, C. *Inorg. Chem.* **2008**, *47*, 3568–3576. (c) Fabelo, O.; Pasán, J.; Cañadillas-Delgado, L.; Delgado, F. S.; Lloret, F.; Julve, M.; Ruiz-Pérez, C. *Inorg. Chem.* **2008**, *47*, 8053–8051. (d) Fabelo, O.; Pasán, J.; Cañadillas-Delgado, L.; Delgado, F. S.; Labrador, A.; Lloret, F.; Julve, M.; Ruiz-Pérez, C. *Cryst. Growth Des.* **2008**, *8*, 3984–3992.
(26) (a) Herrera, J. M.; Bleuzen, A.; Dromzée, Y.; Julve, M.; Lloret, F.; Verdaguer, M. *Inorg. Chem.* **2003**, *42*, 7052–7059. (b) Rodríguez, A.; Sakiyama, H.; Masciocchi, N.; Galli, S.; Gálvez, N.; Lloret, F.; Colacio, E. *Inorg. Chem.* **2005**, *44*, 8399–8406. (c) Mishra, V.; Lloret, F.; Mukherjee, R. *Inorg. Chim. Acta* **2006**, *359*, 4053–4062. (d) Carlin, R. L. *Magnetochemistry*; Springer-Verlag: Berlin, Heidelberg, 1986.

approach that we have reported recently.[27] It is based on a perturbation model where the magnetic coupling only operates between the ground Kramers doublets which are considered as effective spins $S_{eff} = 1/2$. The magnetic interactions in the excited doublets are neglected and thus, their magnetic properties are considered as those of the magnetically isolated ions. The contribution of these excited doublets to the magnetic properties on the ground one is taken into account by a second-order perturbation theory. This introduces a dependence on J, λ, Δ, and α in the Landé factor of the ground doublet (g_0). J is the isotropic exchange interaction, λ is the spin−orbit coupling, α is the orbital reduction factor [defined as $\alpha = kA$, where k considers the reduction of the spin−orbit coupling because of covalency and A is a measure of the crystal-field strength and it takes into account the admixture of the upper $^4T_{1g}(^4P)$ state into the $^4T_{1g}(^4F)$ ground state],[28] and Δ is the energy gap between the singlet $^4A_2$ and doublet ^4E levels because of the splitting of the orbital triplet $^4T_{1g}$ ground state under an axial distortion. All these effects are incorporated into a function named $G(T,J)$ which replaces the value of the g_0 Landé factor of the ground Kramers doublet. This approach is valid in the limit of the weak magnetic coupling as compared to the spin−orbit coupling, $|J/\lambda| < 0.1$, and it allows the analysis of the magnetic data of high-spin Co(II) compounds in the whole temperature range. Following this approach, the Co(II) ions can be treated as effective spin doublets ($S_{eff} = 1/2$) which are related with the real spins ($S = 3/2$) by $S_{eff} = (3/5)S$. For that, the value of g_0 Landé factor of the ground Kramers doublet is substituted by the $G(T,J)$ function, which is calculated as described.[27]

On the basis of the above and from a magnetic point of view, complex **1** can be viewed as quadratic-layers (2D) of ferromagnetically interacting spin doublets. In this respect, the numerical expression derived by Lines [eq 1][29] can be used to analyze the magnetic susceptibility of **1** where $\Theta = 12kT/25|J|$ and the g factor is replaced by the $G(T,J)$ function.

$$\chi_M = 9N\beta^2[G(T,J)]^2/25|J|\{3\Theta + \sum_{n=1-6} C_n/\Theta^{n-1}\}^{-1} \quad (1)$$

being $C_1 = 4$, $C_2 = 2.667$, $C_3 = 1.185$, $C_4 = 0.149$, $C_5 = -0.191$, and $C_6 = 0.001$.

The corresponding analysis of magnetic data (for $T > 5$ K) of **1** through eq 1 leads to the following set of best-fit parameters: $J = +1.2$ cm^{-1}, $\lambda = -124$ cm^{-1}, $\alpha = 1.23$ and $\Delta = 300$ cm^{-1} with $R = 4.5 \times 10^{-5}$ (R is the agreement factor defined as $\sum_i[(\chi_M T)_{obsd,i} - (\chi_M T)_{calcd,i}]^2/\sum_i[(\chi_M)_{obsd,i}]^2$). The theoretical curve (solid line in Figure 7) reproduces quite well the magnetic data in the temperature range 5−300 K. The low value of the $|J/\lambda|$ quotient (0.01) validates the use of the above approach. The value of λ is -170 cm^{-1} for the free-ion, and A assumes limit values of 1.5 and 1.0 for weak and strong crystal-fields, respectively.[28] The values of the λ, A, k, and Δ parameters lie within the range of those observed in other six-coordinated high-spin Co(II) complexes.[26]

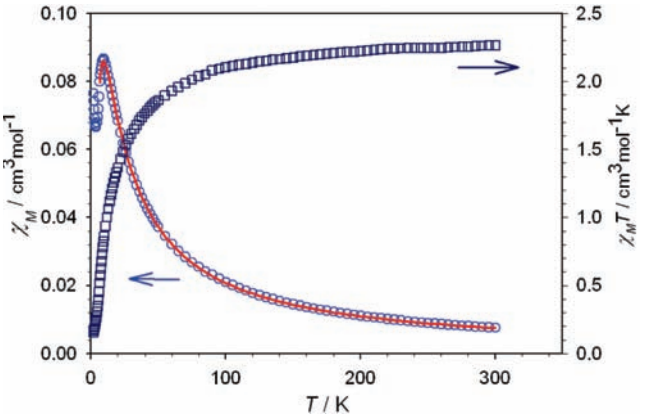

Figure 8. Temperature dependence of χ_M (circles) and $\chi_M T$ (squares) for **2**. The solid line is the best-fit curve through eq 2 (see text).

The intralayer ferromagnetic coupling in **1** ($J = +1.2$ cm^{-1}) is in agreement with the well-known ability of the *anti-syn* carboxylate bridge to mediate weak ferro- and antiferromagnetic interactions,[30,31] features which have been substantiated by density functional theory (DFT) type calculations for dinuclear Cu(II) complexes.[32] However, magneto-structural studies on six-coordinated cobalt(II) complexes with the *anti-syn* carboxylate as a bridge are scarce.[20,25c,33] Examples of weak ferro- [the layered compound $[Co(H_2O)_2(OOCCH_2OC_6H_5)_2]_n$[21] with $J = +0.16$ cm^{-1}] and antiferromagnetic couplings [the 3D compound $[Co_2(bta)(H_2O)_4]_n \cdot 2nH_2O$ with $J = -0.06$ cm^{-1}][25c] are known. The paucity of these data precludes us to go further in our discussion on the magnetic coupling of **1**.

Compound 2. The magnetic properties of compound **2** in the form of the $\chi_M T$ product against T [χ_M being the magnetic susceptibility per mol of Co(II) ions] are shown in Figure 8. At room temperature, $\chi_M T$ is equal to 2.59 cm^3 mol^{-1} K [μ_{eff} per Co(II) = 4.26 μ_B], a value which lies in the lower limit of the range observed for tetrahedral Co(II) complexes [μ_{eff} varying between 4.26 and 4.66 μ_B with the Co(II) in a $^4A_2$ ground state].[34,35] Upon cooling,

(27) Lloret, F.; Julve, M.; Cano, J.; Ruiz-García, R.; Pardo, E. *Inorg. Chim. Acta* **2008**, *361*, 3432–3445.
(28) (a) Figgis, B. N.; Gerloch, M.; Lewis, J.; Mabbs, F. E.; Webb, G. A. *J. Chem. Soc., A* **1968**, 2086–2093. (b) Gerloch, M.; Quested, P. N. *J. Chem. Soc, A* **1971**, 3729–3756. (c) Mabbs, F. E.; Machin, D. J. *Magnetism in Transition Metal Complexes*; Chapman and Hall: London, 1973.
(29) Lines, M. E. *J. Phys. Chem. Solids* **1970**, *31*, 101–116.
(30) (a) Ruiz-Pérez, C.; Sanchiz, J.; Hernández-Molina, M.; Lloret, F.; Julve, M. *Inorg. Chem.* **2000**, *39*, 1363–1370. (b) Rodríguez-Martín, Y.; Hernández-Molina, M.; Delgado, F. S.; Pasán, J.; Ruiz-Pérez, C.; Sanchiz, J.; Lloret, F.; Julve, M. *CrystEngComm* **2002**, *4*, 440–446. (c) Pasán, J.; Sanchiz, J.; Ruiz-Pérez, C.; Campo, J.; Lloret, F.; Julve, M. *Chem. Commun.* **2006**, 2857–2859.
(31) (a) Chattopadhyay, D.; Chattopadhyay, S. K.; Lowe, P. R.; Schawalbe, C. H.; Mazumber, S. K.; Rana, A.; Ghosh, S. *J. Chem. Soc., Dalton Trans.* **1993**, 913–916. (b) Sanchiz, J.; Rodríguez-Martín, Y.; Ruiz-Pérez, C.; Mederos, A.; Lloret, F.; Julve, M. *New J. Chem.* **2002**, *26*, 1624–1628. (c) Pasán, J.; Sanchiz, J.; Ruiz-Pérez, C.; Lloret, F.; Julve, M. *Inorg. Chem.* **2005**, *44*, 7794–7801.
(32) Rodríguez-Fortea, A.; Alemany, P.; Alvarez, S.; Ruiz, E. *Chem.—Eur. J.* **2001**, *7*, 627–637.
(33) Coronado, E.; Drillon, M.; Beltrán, D.; Bernier, J. C. *Inorg. Chem.* **1984**, *23*, 4000–4004.
(34) (a) Reference 20, p 65.(b) Bergman, J. G.; Cotton, F. A. *Inorg. Chem.* **1966**, *5*, 1420–1423.
(35) (a) Carlin, R. L. *Science* **1985**, *227*, 1291–1295. (b) Carlin, R. L. *J. Appl. Phys.* **1981**, *52*, 1993–1997.

$\chi_M T$ continuously decreases to reach a value of 0.15 cm^3 mol^{-1} K at 1.9 K. A maximum of the magnetic susceptibility occurs at 9.5 K, indicating the existence of an antiferromagnetic coupling in **2**.

On the basis of the lack of a significant magnetic coupling between the cobalt(II) ions of **2** through the extended $phda^{2-}$ bridge, most likely the exchange pathway in this compound is provided by *anti-syn* carboxylate bridges within each square layer of cobalt atoms. Consequently, we have treated the magnetic data of **2** through the Lines expression for a square grid of interacting spin quartets [eq 2][29]

$$\chi_M = N\beta^2 g^2/|J|\{3\Theta + \Sigma_{n=1-6} C_n/\Theta^{n-1}\}^{-1} \quad (2)$$

where $\Theta = 4kT/15|J|$, $C_1 = 4$, $C_2 = 1.600$, $C_3 = 0.304$, $C_4 = 0.249$, $C_5 = 0.132$, and $C_6 = 0.013$. Because of the unavailability of a theoretical expression including both the magnetic coupling and the zero field splitting for the square lattice of tetrahedral Co(II) ions, the fit was performed discarding this last parameter. Least-squares fit of the magnetic susceptibility data of **2** in the temperature range 5−300 K through eq 2 leads to following best-fit parameters: $J = -1.63$ cm^{-1}, $g = 2.23$, and $R = 2.6 \times 10^{-5}$ (R is the agreement factor defined as $\sum_i[(\chi_M)_{obsd,i} - (\chi_M)_{calcd,i}]^2/\sum_i[(\chi_M)_{obsd,i}]^2$). The calculated curve reproduces well the magnetic data from room temperature until 5 K. The computed value of the Landé factor for **2** [$g = 2.23$] lies in the range of previous values for this parameter in other tetrahedral Co(II) species (ca. 2.2−2.4). Finally, the obtained antiferromagnetic coupling in **2** agrees with those observed in other layered systems of tetrahedral cobalt(II) ions with the carboxylate bridge in the *anti-syn* bridging mode.[21,36]

Compound 3. The magnetic properties of **3** in the form of the χ_M and $\chi_M T$ against T plots [χ_M being the magnetic susceptibility per mol of Co(II) ions] under an applied magnetic dc field of 1 T are shown in Figure 9. This plot is very close to that observed for the previous compound: $\chi_M T$ continuously decreases from 2.59 cm^3 mol^{-1} K at room temperature ($\mu_{eff} = 4.55\,\mu_B$) to 0.13 cm^3 mol^{-1} K at 1.9 K. A maximum of the magnetic susceptibility occurs at 10.5 K confirming the occurrence of a significant intralayer antiferromagnetic interaction between the tetrahedral cobalt(II) ions in **3**, as observed for **2**.

However, the χ_M versus T plot for **3** exhibits a fast increase below 8.0 K when the applied magnetic field is decreased from 1 T to 50 G (see inset of Figure 9). This abrupt increase of $\chi_M T$ below 8 K is due to a magnetic phase transition related to a spin canting[37] with a critical temperature $T_c = 7.5$ K. Its occurrence is supported by the field-cooled and zero-field cooled magnetizations (inset Figure 9), hysteresis loop and ac susceptibility

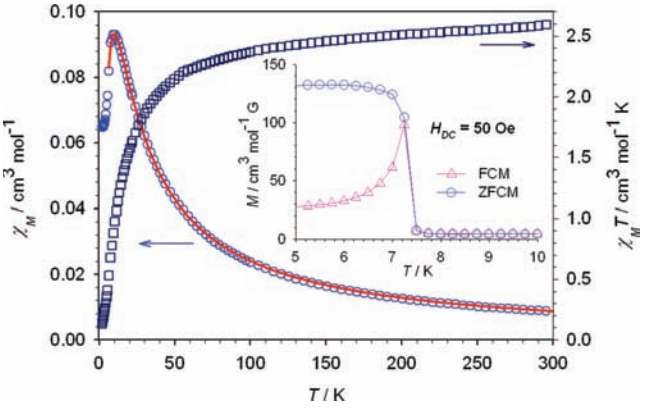

Figure 9. Temperature dependence of χ_M (circles) and $\chi_M T$ (squares) for **3** under an applied magnetic field of 1 T. The solid line is the best-fit curve through eq 2 (see text). The inset shows the field-cooled and zero field-cooled magnetization (the solid lines are guides for the eyes).

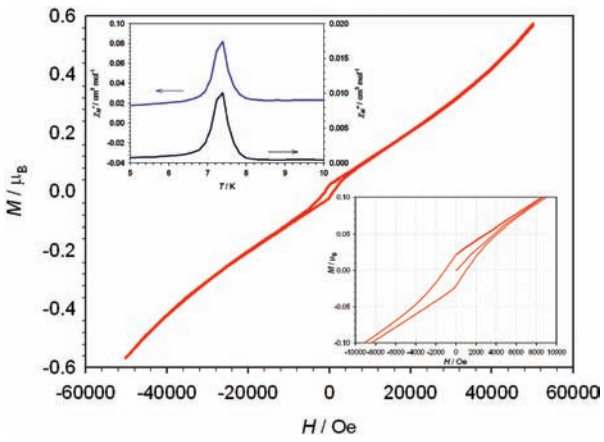

Figure 10. Hysteresis loop of **4** at 2.0 K. The inset shows the temperature dependence of the real (χ'_M) and imaginary (χ''_M) components of the ac susceptibility measured in a zero applied static field and under an oscillating field of ±1 G.

measurements (Figure 10). Upon cooling in a low field ($H = 50$ G), the magnetization of **1** exhibits a sharp transition below 8 K (Figure 9) and then it approaches a saturation value of 135 cm^3 mol^{-1} G (0.024 μ_B). This value is far away from that expected for a high-spin Co(II) ion, indicating the presence of a small canting angle (θ). From this saturation value, a canting angle of about 0.4° with $\theta = 2\sin^{-1}(M_c/2M_s)$. M_c is the saturation value at 50 G and $M_s = gS$ is the expected saturation magnetization if all the moments are ferromagnetically aligned (considering, $g = 2.4$ and $S = 3/2$, see below).[37] The value of T_c is taken here as the maxima observed for in-phase (χ_M') and out-of-phase (χ_M'') ac magnetic susceptibilities (see Figure 10). The magnetic hysteresis loop is shown in Figure 10. The values of coercive field (H_c) and remnant magnetization (M_r) at 2.0 K are 800 G and 0.02 μ_B, respectively.

The exchange pathway for the observed antiferromagnetic coupling within each magnetically isolated square layer of tetrahedral cobalt(II) ions in **3** is provided by the *anti-syn* carboxylato bridge. Consequently, we can analyze the magnetic data of **3** in the temperature range 8−300 K through eq 2. The best-fit parameters are: $J = -1.72$ cm^{-1}, $g = 2.40$, and $R = 2.9 \times 10^{-5}$ (R is the agreement factor defined as $\sum_i[(\chi_M)_{obsd,i} - (\chi_M)_{calcd,i}]^2/\sum_i[(\chi_M)_{obsd,i}]^2$). The calculated curve reproduces the

(36) Lee, E.; Kim, Y.; Jung, D.-Y. *Inorg. Chem.* **2002**, *41*, 501–506.
(37) (a) Marino, N.; Mastropietro, T. F.; Armentano, D.; De Munno, G.; Doyle, R. P.; Lloret, F.; Julve, M. *Dalton Trans.* **2008**, 5152–5154. (b) Armentano, D.; Mastropietro, T. F.; De Munno, G.; Rossi, P.; Lloret, F.; Julve, M. *Inorg. Chem.* **2008**, *47*, 3772–3786. (c) Armentano, D.; De Munno, G.; Mastropietro, T. F.; Julve, M.; Lloret, F. *J. Am. Chem. Soc.* **2005**, *127*, 10778–10779. (d) Armentano, D.; De Munno, G.; Mastropietro, T. F.; Proserpio, D.; Julve, M.; Lloret, F. *Inorg. Chem.* **2004**, *43*, 5177–5179. (e) Armentano, D.; De Munno, G.; Lloret, F.; Palii, A. V.; Julve, M. *Inorg. Chem.* **2002**, *41*, 2007–2013.

magnetic data from room temperature down to 8 K. The value of the antiferromagnetic coupling in **3** is very close to that of **2** because of the identical exchange pathway between the tetrahedral cobalt(II) ions within each square layer in both compounds with shortest values of the intralayer cobalt−cobalt separation of ca. 4.87 (**2**) and 4.68 Å (**3**). The corrugated structure of each layer of cobalt atoms in **3**, where the metal atoms are related by a 2-fold rotation axis in contrast to what occurs in **2** where intralayer inversion centers operate among the non-adjacent cobalt atoms, would account for the spin canting observed in **3**.

Conclusion

Three distinct layered or pillared-layered complexes have been identified in the hydrothermal reaction of Co(II) and 1,4-phenylenediacetic acid or 1,1-cyclohexanediacetic acid in aqueous media: a weak but significant ferromagnetic coupling is present in $[Co(H_2O)_2(phda)]$ (**1**) whereas antiferromagnetic interactions govern the magnetic behavior in [Co(phda)] (**2**) and [Co(chda)] (**3**), the last one exhibiting a spin-canted structure.

The examples presented here are clear cases for which we have demonstrated that small structural modifications may cause important differences in the magnetic behavior of similar systems. In compound **1**, the tilt angle among the adjacent CoO_6 polyhedra together with the fact of *anti-syn* carboxylate bridge is connecting equatorial and axial sites, causes a ferromagnetic coupling within the layers. Because of the lower symmetry of **3** with respect to that of **2**, complex **3** exhibits a spin-canted structure with T_c at about 7.5 K.

Acknowledgment. Funding for this work is provided by the Ministerio Español de Ciencia e Innovación through projects MAT2007-60660, CTQ2007-61690, and "Factoría de Crystalización" (Consolider-Ingenio2010, CSD2006-00015). O.F. thanks the Spanish Ministerio de Ciencia e Innovación for a predoctoral fellowship. L.C.-D. thanks the Gobierno Autónomo de Canarias for a predoctoral fellowship. Thanks are also due to the Project CSD2006-00015 for a postdoctoral contract on behalf of J.P.